

Figure S1 – Deletion analysis of the Mif2-PEST region and phenotypic analysis of associated mutants. Related to Figure 1.

(A) Plasmid-shuffling assay to test the complementation ability of *MIF2* alleles. The chromosomal genotype of the strain was *mif2Δ*. Rescue and test plasmids were *pRS316-MIF2::URA* and *pRS315-mif2::LEU2*, respectively. Numbers correspond to deleted amino acid residues. The diagram at right shows Mif2 residues 1-241 with deleted segments drawn as a dotted line. Viability upon ejection of the *MIF2* rescue plasmid on 5-FOA is shown in the panel at right (+ – growth; - – no growth; +- – intermediate growth phenotype). (B) Growth analysis for strains carrying the indicated *MIF2* alleles integrated into the endogenous *MIF2* locus. Stress conditions are indicated beneath images. (C) FACS analysis of *MIF2* mutants (asynchronous cultures). (D) Measurement of *MIF2* growth phenotypes upon exposure to HU and benomyl. See Figure 1D for related growth assays. *MIF2*, *mif2-10A*, or *mif2-10D* replaced endogenous *MIF2*.

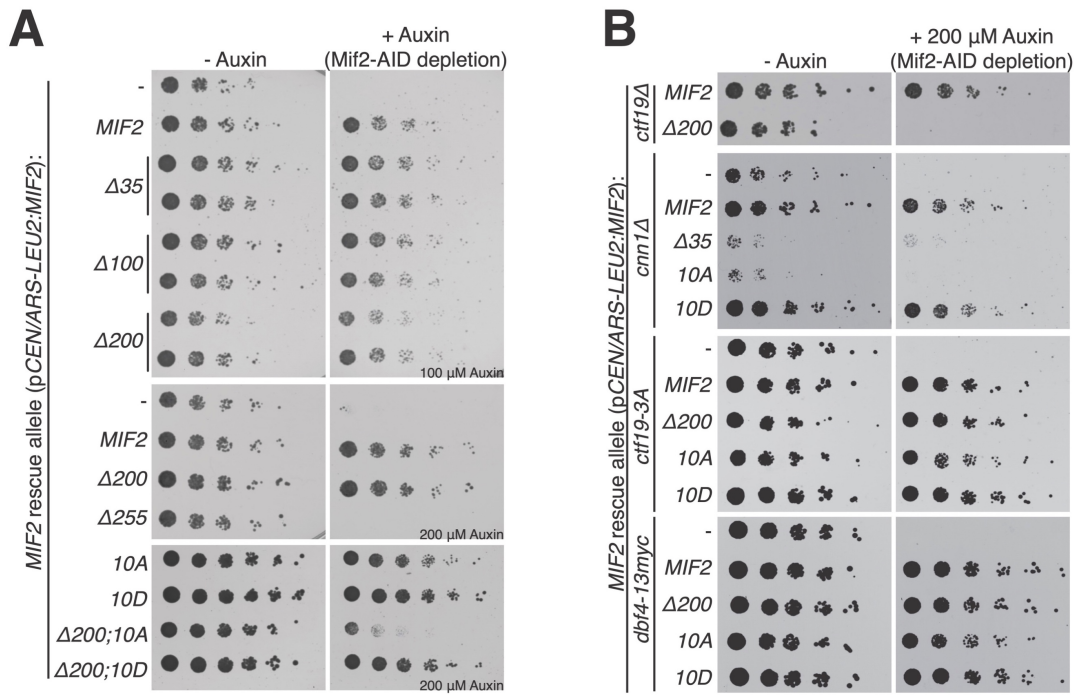


Figure S2 – Mif2 genetic complementation tests and analysis of associated mutants. Related to Figure 1.

(A) Endogenous Mif2 was depleted by auxin treatment, and the indicated *MIF2* alleles were supplied on a centromeric plasmid coding for *MIF2* and ~500 bp flanking chromosomal DNA (*pCEN/ARS-LEU2 MIF2*). These data are summarized in Figure 1A. (B) Complementation analysis as in panel A. The test strain carried *MIF2-AID*, the indicated deletions or mutations shown at left (*ctf19 Δ* , *cnn1 Δ* , *ctf19-3A*, or *dbf3-13myc*), and complementing *MIF2* carried on the same plasmid used for panel A. *ctf19-3A* disrupts centromeric cohesin recruitment. *dbf4-13myc* inactivates early centromere replication. These data are summarized in Figure 1A.

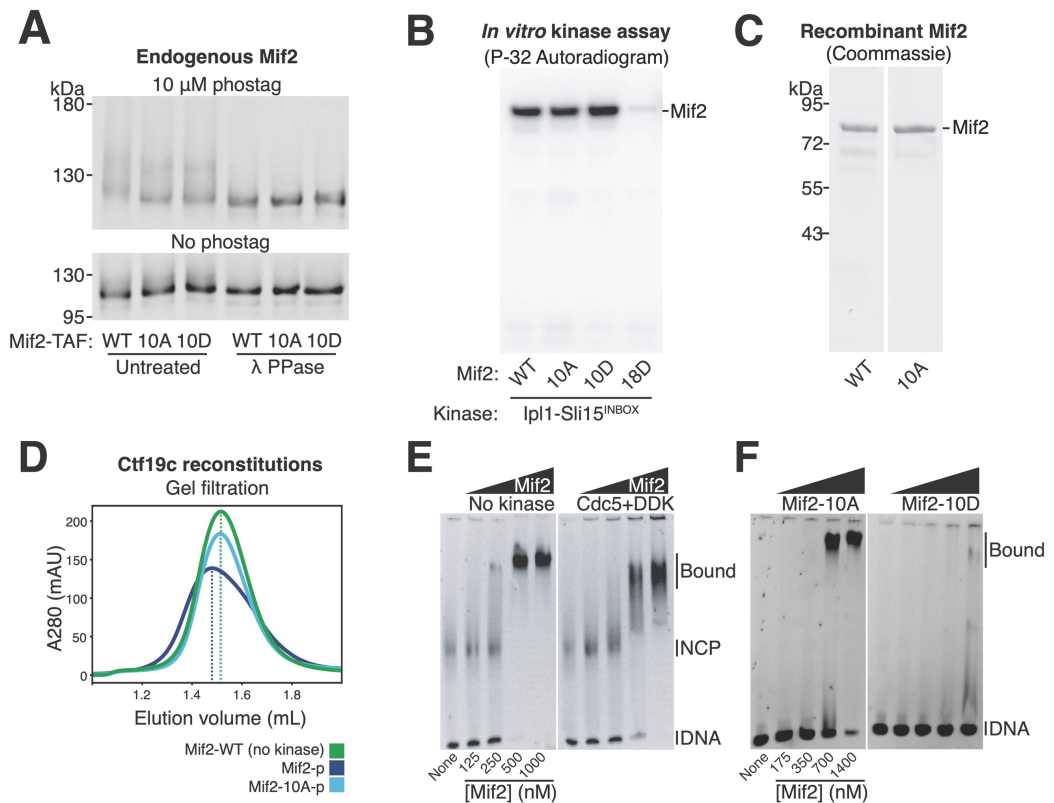


Figure S3 – Further analysis of Mif2 phosphorylation and its biochemical consequence. Related to Figures 1, 2, and 3.

(A) Endogenous Mif2-TAF proteins were immunopurified from asynchronous cultures before incubation with phosphatase buffer (Untreated; left) or lambda phosphatase (λ PPase; right). Reaction products were resolved by SDS-PAGE with 10 μ M (top) or 0 μ M (bottom) Phos-tag acrylamide. Anti-protein A Western blot is shown. (B) Purified full length Mif2-WT, -10A, -10D, or -18D was phosphorylated with recombinant Ipl1. In addition to the 10D substitutions, Mif2-18D has: S53D, S54D, S97D, S98D, S150D, T151D, S154D, T288D. These were identified in MS experiments (Figure 2C). (C) Coomassie-stained gel showing purified Mif2 protein samples used for the experiment shown in Figure 2B. (D) UV absorbance curves also shown in Figure 3 and stacked here for direct comparison. In all experiments, Ctf19c, Mif2, and the Cse4 nucleosome were mixed according to the schematics in Figure 3. The figure shows the elution profiles for the following complexes: green –Mif2-WT-Cse4 nucleosome complex with Ctf19c; dark blue – phosphorylated Mif2-WT-Cse4 nucleosome complex with Ctf19c; light blue – phosphorylated Mif2-10A-Cse4 nucleosome complex with Ctf19c. The vertical dotted lines mark the peak maxima. (E) EMSA showing the interaction between Mif2 and the Cse4 nucleosome. Monomeric Mif2 concentrations are listed below. Mif2 was incubated with ATP (left) or ATP and the indicated kinases (left) before mixing with nucleosome particles. (F) EMSA experiment showing the interaction of the indicated Mif2 proteins with 601 DNA.

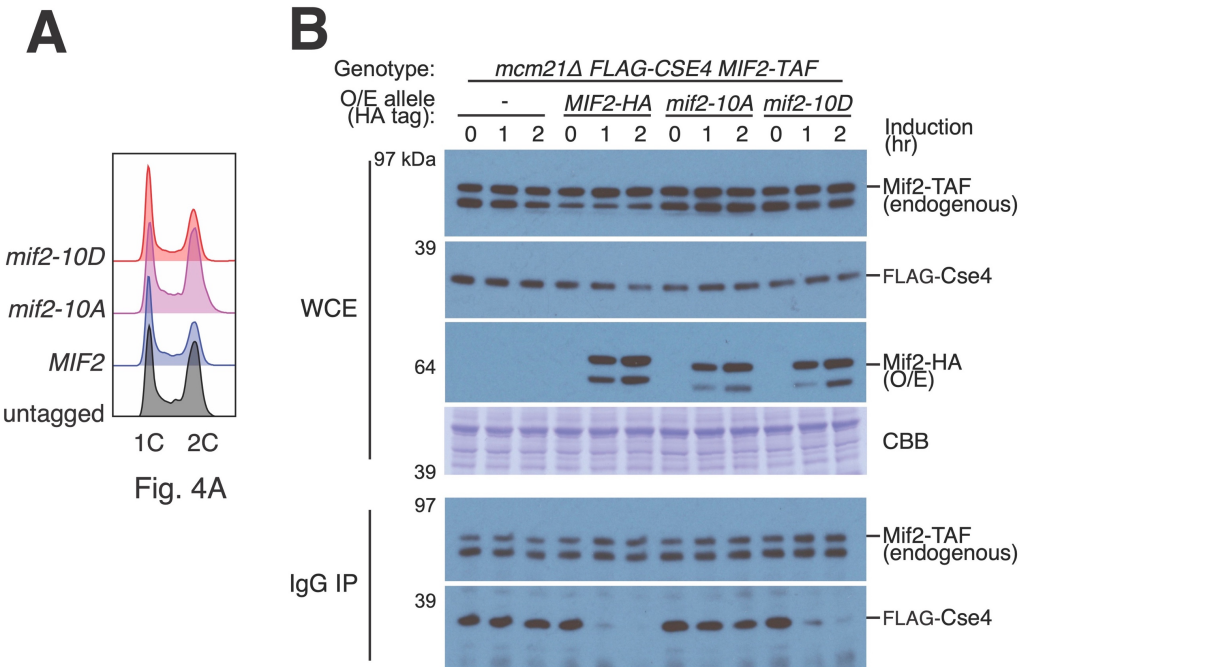
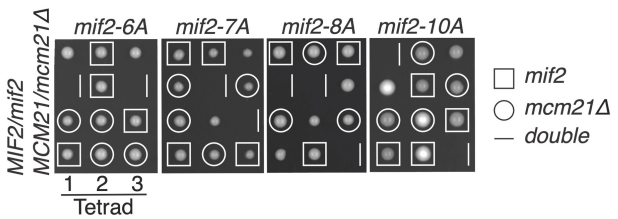
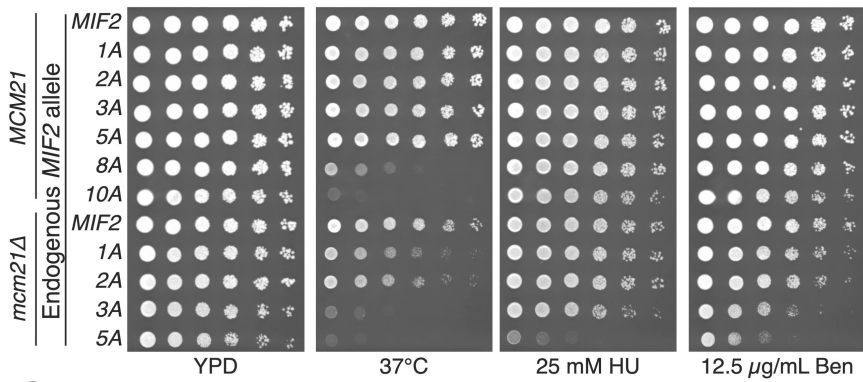
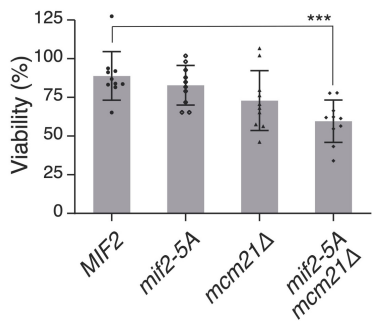


Figure S4 – Overexpressed Mif2-10A failed to compete against endogenous Mif2 in binding Cse4 in cells lacking Mcm21, indicating that the defect of *mif2-10A* is independent of Mcm21. Related to Figure 4.

(A) Cell cycle analysis for cultures used in Figure 4A. Plot show DNA content for asynchronous cultures from the indicated strains. (B) Mif2 competition pulldown experiments were performed as in Figure 4D. The strain genotype was as indicated (*mcm21Δ FLAG-CSE4 MIF2-TAF*). The indicated extragenic *MIF2* alleles were overexpressed.

A**B****C****Viability after Nocodazole release****Figure S5 – Viability of *mif2* and *mcm21* mutant cells. Related to Figure 5.**

(A) Synthetic lethality of the indicated *MIF2* alleles with *mcm21Δ* was assessed by sporulation. Meiotic products of heterozygous diploid strains (*MCM21/mcm21Δ MIF2/mif2*-6A, -7A, -8A, or -10A) are shown. (B) Sensitivity to heat stress (37 °C), replication stress (HU), or spindle stress (Ben) upon successive inactivation of Mif2-PEST phosphorylation sites in *MCM21* or *mcm21Δ* strains. The indicated *MIF2* alleles were integrated at the *MIF2* chromosomal locus. *mif2*-8A and -10A were not tested in *mcm21Δ* cells due to synthetic lethality. Figure 5B shows the positions of the mutations. (C) *mif2-5A mcm21Δ* cells show decreased viability upon release from a nocodazole arrest.

Plasmid	Description
pSMH1409	pRS315 <i>MIF2</i> (chrXI:272,891-275,577)
pSMH1474	pRS315 <i>mif2</i> -Δ35
pSMH1476	pRS315 <i>mif2</i> -Δ100
pSMH1468	pRS315 <i>mif2</i> -Δ200
pSMH1486	pRS315 <i>mif2</i> -Δ256
pSMH1869	pRS315 <i>mif2</i> -14A
pSMH1870	pRS315 <i>mif2</i> -14D
pSMH1495	pRS315 <i>mif2</i> -10A
pSMH1496	pRS315 <i>mif2</i> -10D
pSMH1867	pRS315 <i>mif2</i> -4A
pSMH1868	pRS315 <i>mif2</i> -4D
pSMH1497	pRS315 <i>mif2</i> -Δ200;10A
pSMH1498	pRS315 <i>mif2</i> -Δ200;10D
pSMH1684	pFastBac (438-B) 6xHis-Dbf4; 6xHis-Cdc7-AS3
pSMH1104	pLIC-Tra 6xHis-MBP-Cdc5
pSMH1320	pLIC-Tra 6xHis-Sli15-580-698; 6xHis-Ipl1-AS6
pSMH1172	pFastBac 6xHis-FLAG-Mif2
pSMH1864	pFastBac 6xHis-FLAG-Mif2-10A
pSMH1501	pFastBac 6xHis-FLAG-Mif2-10D
pSMH104	pLIC-Tra 6xHis-TEV-Chl4; 6xHis-TEV-Im13 (Hinshaw and Harrison, 2013)
pSMH1680	pFastBac (438-B) 6xHis-Ame1; Okp1; 6xHis-Nkp1; Nkp2; 6xHis-Ctf19; Mcm21
pSMH1703	pFastBac (438-B) 6xHis-Ctf3; Mcm16; Mcm22; 6xHis-Cnn1; Wip1
pSMH1741	pLIC-Tra 6xHis-Hhf1 (codon optimized); 6xHis-Hta1; Htb1; Hht1 (Addgene #160930)
pSMH1742	pLIC-Tra 6xHis-Hhf1 (codon optimized); 6xHis-Hta1; Htb1; Cse4 (Addgene #160929)
HZE1904	pRS315- <i>MIF2</i> (chrXI:272980-275333)
HZE1905	pRS316- <i>MIF2</i>
HZE1912	pRS315- <i>MIF2-TAF::HisMX</i>
HZE1928	pRS315- <i>mif2</i> -(2-60del)- <i>TAF::HisMX</i>
HZE1932	pRS315- <i>mif2</i> -(61-240del)- <i>TAF::HisMX</i>
HZE1933	pRS315- <i>mif2</i> -(61-101del)- <i>TAF::HisMX</i>

HZE1934	pRS315- <i>mif2</i> -(102-240del)-TAF::HisMX
HZE1936	pRS315- <i>mif2</i> -(181-240del)-TAF::HisMX
HZE1938	pRS315- <i>mif2</i> -(61-180del)-TAF::HisMX
HZE1939	pRS315- <i>mif2</i> -(61-210del)-TAF::HisMX
HZE1940	pRS315- <i>mif2</i> -(211-240del)-TAF::HisMX
HZE2941	pRS315- <i>mif2</i> -10A-TAF::HisMX, 10A (S217A, S226A, S228A, S229A, S232A, S234A, S236A, S238A, S240A, T245A)
HZE2942	pRS315- <i>mif2</i> -10D-TAF::HisMX, 10D (S217D, S226D, S228D, S229D, S232D, S234D, S236D, S238D, S240D, T245D)
HZY1569	pRS425-GAL1-10
HZY1924	pRS425-GAL1-10- <i>Mif2</i> -6xHIS-3xHA
HZY2979	pRS425-GAL1-10- <i>mif2</i> -10A-6xHIS-3xHA
HZE3048	pRS315- <i>mif2</i> -S217A-TAF::HisMX
HZE3049	pRS315- <i>mif2</i> -3SA(S226A, S228A and S229A)-TAF::HisMX
HZE3050	pRS315- <i>mif2</i> -T245A-TAF::HisMX
HZE3067	pRS315- <i>mif2</i> -S226A-TAF::HisMX
HZE3068	pRS315- <i>mif2</i> -2SA(S228A and S229A)-TAF::HisMX
HZE3069	pRS315- <i>mif2</i> -5SA(S232A, S234A, S236A, S238A, S240A)-TAF::HisMX
HZE3070	pRS315- <i>mif2</i> -8SA(S226A, S228A, S229A, S232A, S234A, S236A, S238A, S240A)-TAF::HisMX
HZE3153	pRS315- <i>mif2</i> -6SA(S226A, S232A, S234A, S236A, S238A, S240A)-TAF::HisMX
HZE2154	pRS315- <i>mif2</i> -7SA(S228A, S229A, S232A, S234A, S236A, S238A, S240A)-TAF::HisMX

Table S1 – Plasmids used in this work.

Strain Number	Genotype	Figure/Source
AM7579	W303 MATa <i>ura3::pADH1-OsTIR1-9MYC::URA3</i>	Adèle Marston
SMH614	MATa <i>ura3::pADH1-OsTIR1-9MYC::URA3 MIF2-3xHA-IAA7::KanMX</i>	Fig. 1, S1
SMH619	MATa <i>ura3::pADH1-OsTIR1-9MYC::URA3 MIF2-3xHA-IAA7::KanMX ctf19Δ::HISMX</i>	Fig. 1, S1
SMH629	MATa <i>ura3::pADH1-OsTIR1-9MYC::URA3 MIF2-3xHA-IAA7::KanMX cnn1Δ::HISMX</i>	Fig. 1, S1
SMH625	MATa <i>ura3::pADH1-OsTIR1-9MYC::URA3 MIF2-3xHA-IAA7::KanMX ctf19-3A::HISMX</i>	Fig. 1, S1
SMH833	MATa <i>ura3::pADH1-OsTIR1-9MYC::URA3 MIF2-3xHA-IAA7::KanMX dbf4-18myc::TRP1</i>	Fig. 1, S1
HZY366	W303 MATa <i>mif2Δ::NAT pRS316-MIF2</i>	Fig. 1C, S1
HZY1247	W303 MATa <i>mcm21Δ::KanMX mif2Δ::NAT pRS316-MIF2/MCM21</i>	Fig. 1C
HZY1616	S288c MATa <i>bar1Δ::URA3 sml1Δ::TRP1</i>	Fig. 1D, S1
HZY1681	S288c MATa <i>mif2-10A-TAF::HisMX bar1Δ::URA3 sml1Δ::TRP1</i>	Fig. 1D, S1
HZY1682	S288c MATa <i>mif2-10D-TAF::HisMX bar1Δ::URA3 sml1Δ::TRP1</i>	Fig. 1D, S1
HZY3490	S288c MATa <i>MIF2-TAF::HisMX sml1Δ::TRP1</i>	Fig. S1
HZY3499	S288c MATa <i>mif2-2-60del-TAF::HisMX sml1Δ::TRP1</i>	Fig. S1
HZY3504	S288c MATa <i>mif2-61-240del-TAF::HisMX sml1Δ::TRP1</i>	Fig. S1
HZY3507	S288c MATa <i>mif2-61-101del-TAF::HisMX sml1Δ::TRP1</i>	Fig. S1
HZY3526	S288c MATa <i>mif2-102-240del-TAF::HisMX sml1Δ::TRP1</i>	Fig. S1

HZY3514	S288c MATa <i>mif2-61-180del-TAF::HisMX sml1Δ::TRP1</i>	Fig. S1
HZY3522	S288c MATa <i>mif2-181-240del-TAF::HisMX sml1Δ::TRP1</i>	Fig. S1
HZY3537	S288c MATa <i>mif2-61-210del-TAF::HisMX sml1Δ::TRP1</i>	Fig. S1
HZY3538	S288c MATa <i>mif2-211-240del-TAF::HisMX sml1Δ::TRP1</i>	Fig. S1
SCY249	S288c MATa <i>sml1Δ::TRP1 arg4Δ</i>	Fig. 4A
HZY1620	S288c MATa <i>MIF2-TAF::HisMX sml1Δ::TRP1 bar1Δ::URA3</i>	Fig. 1E, 4A, S3A
HZY1681	S288c MATa <i>mif2-10A-TAF::HisMX sml1Δ::TRP1 bar1Δ::URA3</i>	Fig. 1E, 4A, S3A
HZY1682	S288c MATa <i>mif2-10D-TAF::HisMX sml1Δ::TRP1 bar1Δ::URA3</i>	Fig. 1E, 4A, S3A
HZY1847	S288c MATa <i>3xFLAG-CSE4::KanMX MIF2-TAF::HisMX bar1Δ::URA3 sml1Δ::TRP1</i>	Fig. 4C, 5AC
HZY1849	S288c MATa <i>3xFLAG-CSE4::KanMX mif2-10A-TAF::HisMX bar1Δ::URA3 sml1Δ::TRP1</i>	Fig. 4B
HZY1173	S288c MATa <i>3xFLAG-CSE4::KanMX MIF2-TAF::HisMX mcm21Δ::Hyg bar1Δ::URA3</i>	Fig. S4B
HZY1685	W303 MATa <i>LEU2 MIF2-TAF::HisMX</i>	Fig. 5A
HZY1686	W303 MATa <i>LEU2 mif2-10A-TAF::HisMX</i>	Fig. 5A
HZY1688	W303 MATa <i>LEU2 mif2-10D-TAF::HisMX</i>	Fig. 5A
HZY850	W303 MATa <i>LEU2 mcm21Δ::KanMX</i>	Fig. 5A
HZY1016	W303 Diploid (<i>mif2-10A-TAF::HisMX/MIF2 mcm21Δ::Hyg/MCM21 bar1Δ::KanMX/BAR1</i>)	Fig. S5A
HZY1026	W303 Diploid (<i>mif2-8A-TAF::HisMX/MIF2 mcm21Δ::Hyg/MCM21</i>)	Fig. S5A

HZY2078	W303 Diploid (<i>mif2-6A-TAF::HisMX/MIF2 mcm21Δ::Hyg/MCM21</i>)	Fig. S5A
HZY2079	W303 Diploid (<i>mif2-7A-TAF::HisMX/MIF2 mcm21Δ::Hyg/MCM21</i>)	Fig. S5A
HZY1594	W303 MAT α <i>MIF2-TAF::HisMX</i>	Fig. 5C, S5B-C
HZY2227	W303 MAT α <i>mif2-S217A-TAF::HisMX</i>	Fig. S5B
HZY2228	W303 MAT α <i>mif2-2A-TAF::HisMX</i> (S228A, S229A)	Fig. S5B
HZY2072	W303 MAT α <i>mif2-3A-TAF::HisMX</i> , 3A (S226A, S228A, S229A)	Fig. S5B
HZY2154	W303 MAT α <i>mif2-5A-TAF::HisMX</i> , 5A (S232A, S234A, S236A, S238A, S240A)	Fig. 5C, S5B-C
HZY1437	W303 MAT α <i>mif2-10A-TAF::HisMX</i> , 10A (S217A, S226A, S228A, S229A, S232A, S234A, S236A, S238A, S240A, T245A)	Fig. S5B
HZY1176	W303 MAT α <i>MIF2-TAF::HisMX6 mcm21Δ:Hygro</i>	Fig. 5C, S5B-C
HZY2245	W303 MAT α <i>mif2-S226A -TAF::HisMX6 mcm21Δ:Hygro</i>	Fig. S5B
HZY2247	W303 MAT α <i>mif2-2A-TAF::HisMX6 mcm21Δ:Hygro</i>	Fig. S5B
HZY2102	W303 MAT α <i>mif2-3A-TAF::HisMX6 mcm21Δ:Hygro</i>	Fig. S5B
HZY2208	W303 MAT α <i>mif2-5A-TAF::HisMX6 mcm21Δ:Hygro</i>	Fig. 5C, S5B-C

Table S2 – Yeast strains used in this study. Related to figures 1, 4-5 as indicated.